Available online at www.sciencedirect.com

SCIENCE DIRECT

Journal of Crystal Growth 267 (2004) 8–16

JOURNAL OF CRYSTAL GROWTH

www.elsevier.com/locate/jcrysgro

Thermodynamic modeling of AlGaInN growth by MOVPE

Jindřich Leitner[a,]*, Josef Stejskal[b], Petr Voňka[c]

[a] Department of Solid State Engineering, Institute of Chemical Technology, Technická 5, 166 28 Prague 6, Czech Republic
[b] Department of Inorganic Chemistry, Institute of Chemical Technology, Technická 5, 166 28 Prague 6, Czech Republic
[c] Department of Physical Chemistry, Institute of Chemical Technology, Technická 5, 166 28 Prague 6, Czech Republic

Received 16 January 2003; accepted 8 March 2004
Communicated by K. Nakajima

Abstract

A detailed thermodynamic analysis of the system Al–Ga–In–N–C–H was performed using the Gibbs energy minimization method. The multicomponent gaseous phase, ternary liquid alloy of A^{III} elements, solid solution of A^{III} nitrides as well as graphite and Al_4C_3 were included into the calculation. The influence of the initial conditions, namely temperature, pressure and input gas phase composition, on the equilibrium composition of this system was in view. On the basis of the concept of local equilibrium between the growing layer and the gaseous phase in its close vicinity, the calculated results were used to optimize deposition parameters for MOVPE growth of (Al,Ga,In)N epitaxial layers.
© 2004 Elsevier B.V. All rights reserved.

PACS: 05.70.−a; 81.05.Ea; 81.15.Kk

Keywords: A1. Deposition diagrams; A1. Thermodynamic analysis; A3. Metalorganic vapor phase epitaxy; B1. Nitrides

---

1. Introduction

A^{III} nitrides (AlN, GaN and InN) and their solid solutions ((Al,Ga)N, (Al,In)N, (Ga,In)N and (Al,Ga,In)N) are very important materials with many applications in optoelectronics (light emitting diodes, laser diodes, photodetectors) and electronics (high-power and high-temperature devices) [1–3]. Various methods are utilized for deposition of epitaxial layers and structures of these materials: chloride vapor phase epitaxy (VPE), metalorganic vapor phase epitaxy (MOVPE), molecular beam epitaxy (MBE) or chemical beam epitaxy (CBE). MOVPE has some advantages over other techniques and it became the leading epitaxial technology in the last decade [4–6].

Thermodynamics, fluid dynamics, and gas and surface reactions, all play a part in the deposition process. Thermodynamic aspects of MOVPE were first discussed by Stringfellow [7,8] who demonstrated usefulness of equilibrium calculations for the optimization of deposition conditions. A number of papers dealing with the thermodynamic analysis of A^{III} nitride deposition systems has been published since: AlN [9], GaN [9–11], InN [9], (Al,Ga)N [12–15], (Al,In)N [12,16,17], (Ga,In)N [12,18–23] and (Al,Ga,In)N [24]. When calculating the solid (Ga,In)N composition in the system

---

*Corresponding author. Fax: +420-2-2431-0337.
Email-address: jindrich.leitner@vscht.cz (J. Leitner).

doi:10.1016/j.jcrysgro.2004.03.027

$(CH_3)_3Ga–(CH_3)_3In–NH_3–H_2$, Koukitu et al. [18] introduced an empirical parameter representing non-equilibrium decomposition of ammonia in the gaseous phase. This kinetic restriction and the relevant "quasi-equilibrium" model has been accepted by most of the investigators.

The goal of this work is the detailed thermodynamic analysis of the system Al–Ga–In–N–C–H relevant to the (Al,Ga,In)N growth by the MOVPE. Two main topics are as follows: (1) under which conditions the required solid (namely (Al,Ga,In)N) is the only stable condensed phase and (2) how the temperature, pressure and initial gas phase composition affect the equilibrium composition of this solid. Our calculations differ from the previous work by Koukitu et al. [24] in the following items: (1) no kinetic restriction is assumed, (2) the multicomponent gaseous phase is taken into account in the equilibrium, (3) possible formation of a liquid alloy is considered, (4) reliable thermodynamic data for solid GaN and InN are used and (5) phase separation in highly non-ideal (Al,Ga,In)N solid solution is taken into account.

2. Calculation method

The non-stoichiometric method based on minimization of the total Gibbs energy of the system on the set of points satisfying the material balance conditions was used for the calculation of equilibrium composition of the above-mentioned heterogeneous system. The calculation algorithm and the computer program CHEMEQ were described elsewhere [25].

3. System description and input thermodynamic data

As precursors of A^{III} elements, trimethyl (TM) or triethyl (TE) derivatives are generally used. Ammonia is frequently used as the source of nitrogen although other compounds (e.g. trimethylamine, hydrazine or dimethylhydrazine) have been utilized. Hydrogen or nitrogen are applied as the carrier gas. Metalorganic compounds are unstable at elevated temperatures and decompose in the gas phase or at the gas–solid interface. The decomposition, which was observed experimentally using various analytical techniques, leads to the formation of a number of gaseous species. Therefore, the following gaseous substances were included into the calculation: Al, Al_2, AlH, AlH_2, AlH_3, $AlCH_3$, $Al(CH_3)_2$, $Al(CH_3)_3$, AlN, Ga, Ga_2, GaH, GaH_2, GaH_3, $GaCH_3$, $Ga(CH_3)_2$, $Ga(CH_3)_3$, GaN, In, In_2, InH, InH_2, InH_3, $InCH_3$, $In(CH_3)_2$, $In(CH_3)_3$, InN, N, N_2, N_2H_2, N_2H_4, NH, NH_2, NH_3, H, H_2, HCN, CH_4, C_2H_2, C_2H_4, C_2H_6, CN and C_2N_2. Ideal behavior of the gas phase was assumed. Thermodynamic data for gaseous species were taken from various sources [26–29]. The consistent set of thermodynamic data for the gaseous species in the system A^{III}–N–C–H has been collected recently [30]. There are certain differences between these two data sets but the largest ones concern the less-stable species. In this case the data change does not influence significantly the calculated results.

Depending on the initial conditions, various condensed phases can exist in equilibrium with the gas phase. In the system Al–Ga–In–N–C–H, ternary metallic liquid (Al–Ga–In), solid nitride (Al,Ga,In)N, carbide Al_4C_3 as well as graphite were taken into account. A liquid alloy was described as a substitutional solution and the Redlich-Kister equation was used to express the excess Gibbs energy. The thermodynamic data for pure liquid elements were taken from the SGTE [31] and the Redlich-Kister parameters were taken from the assessment by Ansara et al. [29]. The solubility of nitrogen in the alloy is very low and was neglected in the calculations.

For thermodynamic description of mixed nitride, the sublattice model was used. As the mixing occurs on one sublattice only, this description is equivalent to the pseudoternary AlN–GaN–InN substitutional solution model. The data for pure solid AlN were taken from tables [27]. The data assessed by Leitner et al. [10,21] were used for pure solid GaN and InN. Large discrepancies exist between the thermodynamic data for solid GaN and InN published in the literature. The following values of the standard molar Gibbs energy at temperature of 1000 K are presented for illustration: $G_m^0(\mathrm{GaN}) = -160.9\,\mathrm{kJ/mol}$ [27,33], -173.0 [30], -176.6 [32], -207.9 [10] and $G_m^0(\mathrm{InN}) = -203.9\,\mathrm{kJ/mol}$ [27], -83.0 [33], -140.5 [31], -197.3 [21]. The recently obtained value of the heat of formation of GaN at 298.15 K, $\Delta H_f^0(298.15) = -156.8 \pm 16.0\,\mathrm{kJ/mol}$ [34] confirms our assessed data [10]. One can calculate $G_m^0(\mathrm{GaN}) = -162.7\,\mathrm{kJ/mol}$ and $G_m^0(\mathrm{InN}) = -83.4\,\mathrm{kJ/mol}$ at 1000 K from the data selected by Koukitu et al. [9]. Thus, the calculated values of the equilibrium constant K_{R1} for the exchange reaction

$$\mathrm{GaN(s) + In(g) = InN(s) + Ga(g)} \qquad \text{(R1)}$$

at 1000 K are 4.9×10^{-3} and 1.3×10^{-6} using our selected data and the data accepted by Koukitu et al. [9], respectively. Under the condition that $p(\mathrm{Ga}) = p(\mathrm{In})$, the equilibrium constant of reaction (R1) is equal to the ratio of equilibrium activity of InN and GaN, $a(\mathrm{InN})/a(\mathrm{GaN})$. The large discrepancy in order of magnitude between two values of K_{R1} should cause significant differences in the calculated equilibrium composition of the mixed nitrides (Ga,In)N and (Al,Ga,In)N.

It has been observed [35,36] that the limited mutual solubility region exists in the pseudobinary GaN–InN system. As differences between the lattice parameters of components give rise to this phase separation, the conclusion was made that this phenomenon will occur in other systems containing indium, namely (Al,In)N and (Al,Ga,In)N. The boundary of the two-phase region as well as the spinodal lines for (Al,Ga,In)N were calculated by various authors on the basis of strictly regular solution approximation [35–39]. Relevant interaction parameters were obtained according to the Stringfellow's DLP model [35–38] or by the valence force field model [39]. Deviation from ideal mixing was expressed by the Redlich-Kister equation in this work and corresponding parameters were obtained on the basis of the empirical estimation [40]. Koukitu et al. [24] used the DLP model in their thermodynamic analysis. For the pseudobinary GaN–InN, the interaction parameter $\Omega_{\mathrm{GaN-InN}} = 29.3\,\mathrm{kJ/mol}$ was used [24], which results in the critical temperature $T_C = 1761\,\mathrm{K}$ at $x_{\mathrm{InN}} = 0.5$. Our data lead to $T_C = 2053\,\mathrm{K}$ at $x_{\mathrm{InN}} = 0.43$. Theoretical studies on the GaN–InN system [41–44] lead to the value of T_C in the range 1290–3190 K at $x_{\mathrm{InN}} = 0.39 - 0.5$.

As the solid solution (Al,Ga,In)N exhibits large positive deviations from ideal behavior and as the homogeneous phase is unstable under the most conditions studied, its decomposition into two phases of different compositions was supposed.

The thermodynamic data for solid carbide $\mathrm{Al_4C_3}$ and graphite were taken from tables [27].

4. Results and discussion

The equilibrium composition of the system Al–Ga–In–N–C–H was calculated at temperatures of 700°C, 800°C, and 900°C and relative pressures $p/p^0 = 1$, 0.1 and 0.01 (p is pressure and p^0, $p^0 = 101.325\,\mathrm{kPa}$, is standard pressure). Trimethylaluminium (TMAl), trimethylgallium (TMGa), trimethylindium (TMIn), ammonia, and hydrogen or nitrogen were considered as the input gaseous species. The calculations were performed for various V/III input ratios ($\mathrm{V/III} = n^0(\mathrm{NH_3})/\sum n^0(\mathrm{A^{III}})$, $\sum n^0(\mathrm{A^{III}}) = n^0(\mathrm{TMAl}) + n^0(\mathrm{TMGa}) + n^0(\mathrm{TMIn})$) using the fixed value of $\sum n^0(\mathrm{A^{III}}) = 10^{-5}\,\mathrm{mol}$ for the all of them. As common practice, only the input amount of ammonia was considered for the V/III ratio although the crucial portion of nitrogen is introduced by the carrier gas in $\mathrm{N_2}$ ambient. So the calculated results for the same V/III ratio for $\mathrm{H_2}$ and $\mathrm{N_2}$ carrier gases are incomparable from the thermodynamic point of view. The relative initial contents of $\mathrm{A^{III}}$ elements in the gaseous phase $x^0(\mathrm{A^{III}})$ ($x^0(\mathrm{A^{III}}) = n^0(\mathrm{TMA^{III}})/\sum n^0(\mathrm{A^{III}})$) were changed in the range from 0 to 1. The total initial amount of gases was set to 1 mol in all cases.

4.1. Deposition diagrams

The deposition diagrams show the condensed phase(s), which is (are) stable in equilibrium with the gaseous phase. Such a set of temperature, total pressure and initial gas phase composition, under which the solid nitride (Al,Ga,In)N is the only stable condensed phase, is generally suitable for quality epitaxial layers growth. For correct determination of the (solid nitride)–(solid nitride + liquid alloy) phase boundary, the phase separation in (Al,Ga,In)N has to be taken into account. Let us take as an example $Al_{0.3}Ga_{0.5}In_{0.2}N$ at 800°C under the N_2 atmosphere. If the separation is not considered, the decomposition of solid nitride to liquid alloy and gaseous nitrogen occurs. In opposite case, the phase separation in solid nitride takes place and two solids having composition $Al_{0.372}Ga_{0.614}In_{0.014}N$ and $Al_{0.006}Ga_{0.032}In_{0.963}N$ occur and no liquid alloy is present in equilibrium.

The calculated deposition diagrams for the system Al–Ga–In–N–C–H at $p/p^0 = 1$, V/III = 10000 in hydrogen ambient are shown in Fig. 1. A large (solid + liquid) region exists at temperature of 800°C. Nitride field expansion occurs at lower temperatures (due to the nitride stability increase) as well as at higher temperatures (due to the enhanced evaporation of the liquid alloy). Influence of the total pressure at $t = 800°C$ and V/III = 10000 is demonstrated in Fig. 2. Reduction of the total pressure leads to solid nitride field enlargement as the evaporation of the liquid alloy is enhanced. Decrease of the input V/III ratio affects the solid–(solid + liquid) boundary insignificantly at temperature of 800°C and atmospheric pressure and becomes more important in case of reduced pressure (see Fig. 3).

The situation is quite different in the nitrogen ambient due to the suppression of the decomposition reactions

$$A^{III}N(s) = A^{III}(s,l) + 1/2N_2(g) \qquad \text{(R2)}$$

The solid nitride field is dominant in the temperature range of 700–900°C under atmospheric or reduced pressure and the liquid alloy appears only in limited cases near the TMIn corner. On the other hand graphite formation is possible due to decomposition of methane

$$CH_4(g) = C(s) + 2H_2(g) \qquad \text{(R3)}$$

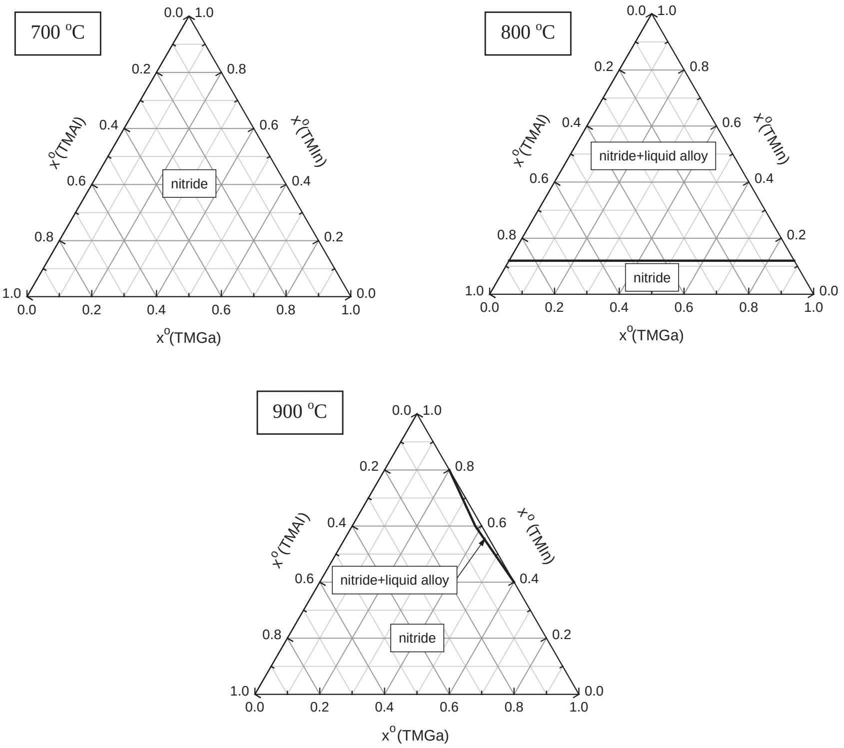

Fig. 1. Deposition diagrams for system Al–Ga–In–N–C–H at $p/p^0 = 1$, V/III = 10^4 in H_2 carrier gas for temperatures of 700°C, 800°C and 900°C.

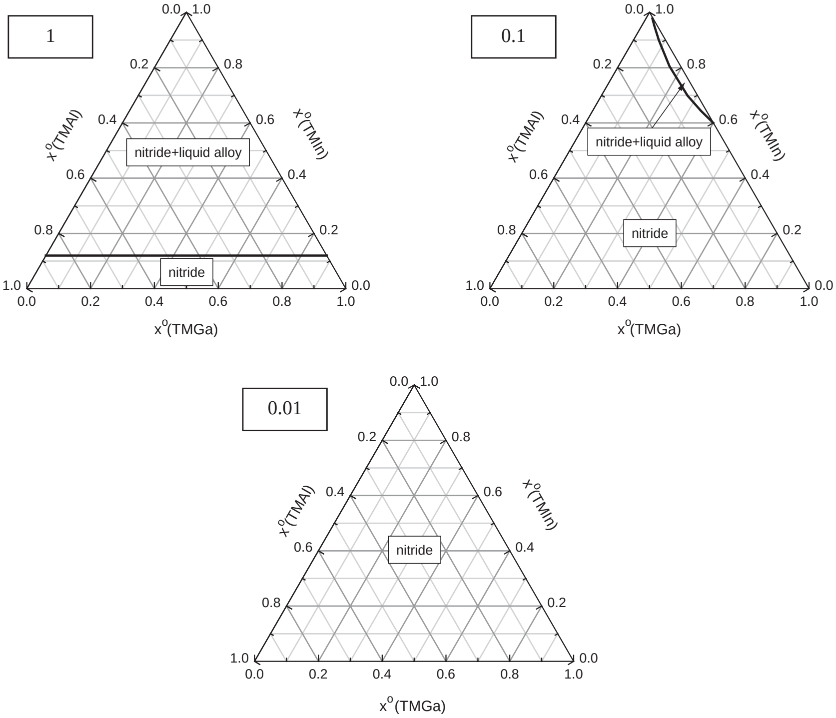

Fig. 2. Deposition diagrams for system Al–Ga–In–N–C–H at $t = 800°\mathrm{C}$, V/III = 10^4 in H_2 carrier gas relative total pressures (p/p^0) 1, 0.1 and 0.01.

The values of the equilibrium constant K_{R3} are 7.69, 21.78 and 52.06 at the temperatures of 700°C, 800°C and 900°C, respectively. One can suppose that the methane partial pressure is equal to triple of the sum of initial partial pressures of trimethylcompounds of A^{III} elements. Thus, the hydrogen partial pressure, which prevents from a graphite formation should be 0.015 (700°C), 0.0256 (800°C) and 0.0395 (900°C) at $\sum p^0(A^{III}) = 10^{-5}$. If nitrogen is used as the carrier gas, limiting values of the V/III input ratio can be roughly estimated as 1012, 1704 and 2634 at the temperature of 700°C, 800°C and 900°C, respectively.

4.2. Solid nitride composition

The calculated average solid nitride compositions at V/III = 10^4 and $x^0(A^{III}) = 1/3$ for various temperatures and total pressures and N_2 carrier gas are shown in Table 1. Average molar fractions of $A^{III}N$ in the solid phase is calculated from the relation

$$x(A^{III}N) = \frac{n'(A^{III}N) + n''(A^{III}N)}{n'_{tot} + n''_{tot}}, \tag{1}$$

where superscripts ′ and ″ denote the first and the second phases of the (Al,Ga,In)N solid solution and n_{tot} the total amount of these phases, respectively. Equilibrium fractions of A^{III} elements in the gaseous phase, $R(A^{III})$, calculated according to the relation

$$R(A^{III}) = \frac{n_g(A^{III})}{n(A^{III})} \tag{2}$$

are also included. It is obvious that the rising temperature and the decreasing pressure lead to significant reduction of the indium content in solid nitride. The influence of temperature can be explained by the lower thermodynamic stability of InN in comparison with GaN and AlN. Indium in the gaseous phase is usually represented by In(g) and InH(g). But it is necessary to underline that

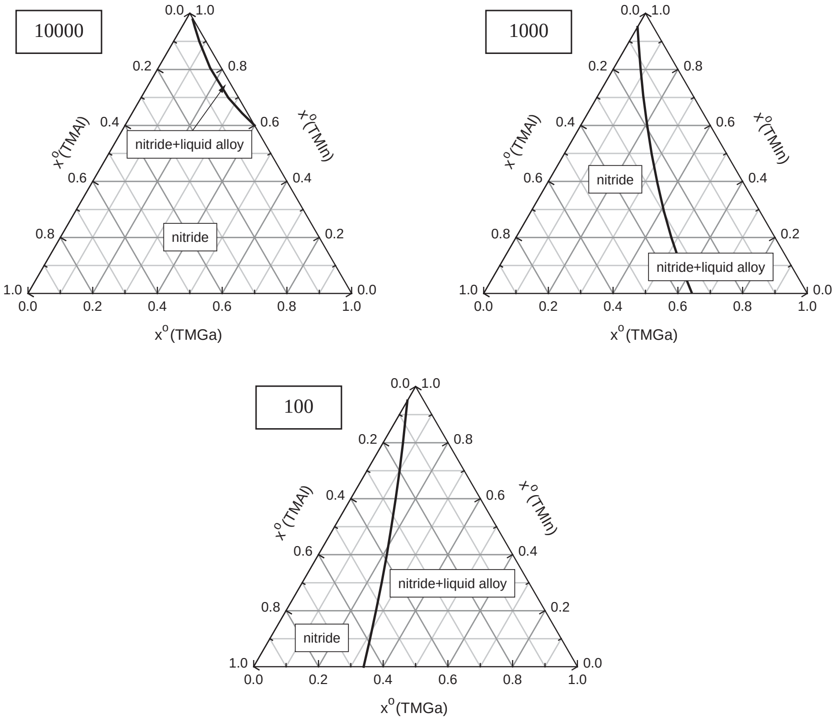

Fig. 3. Deposition diagrams for system Al–Ga–In–N–C–H at $t = 800°C$, $p/p^0 = 0.1$ in H_2 carrier gas for input V/III ratio 10000, 1000 and 100.

Table 1
Calculated solid nitride composition, $x(A^{III}N)$, and equilibrium fraction of A^{III} elements in the gaseous phase, $R(A^{III})$, at $V/III = 10^4$, $x^0(TMA^{III}) = 1/3$, and N_2 carrier gas

		$p = 1$		$p = 0.1$		$p = 0.01$	
		$x(A^{III}N)$	$R(A^{III})(\%)$	$x(A^{III}N)$	$R(A^{III})(\%)$	$x(A^{III}N)$	$R(A^{III})(\%)$
700°C	Al	0.334	1.80E−12	0.340	1.80E−11	0.500	1.60E−10
	Ga	0.334	4.90E−03	0.339	0.05	0.496	0.65
	In	0.333	0.19	0.321	5.38	0.004	99.2
800°C	Al	0.347	4.40E−10	0.505	4.20E−09	0.190	2.00E−08
	Ga	0.346	0.21	0.492	2.7	0.381	38.5
	In	0.307	11.4	0.003	99.4	0.000	100
900°C	Al	0.513	4.30E−08	0.704	4.40E−07	0.979	3.00E−06
	Ga	0.483	5.8	0.296	57.9	0.021	97.9
	In	0.004	99.2	0.000	100	0.000	100

the stability of gaseous species depends significantly on the considered reaction conditions (temperature, pressure and initial composition). Therefore the inclusion of many gaseous species into the calculation is very useful because in advance we do not know which of them will be significant or not. The pressure dependence is not so straightforward and is connected with different stabilities of various A^{III} species in the gaseous phase in equilibrium with solid nitride. Calculated results further show, that in nitrogen ambient it is possible to reach any composition of solid nitride when varying the input number of moles of A^{III} precursors at temperatures of 700–800°C under atmospheric or slightly reduced pressure.

Similar calculations performed for H_2 carrier gas revealed that the indium incorporation efficiency is significantly reduced in this case and higher indium content in solid nitride can be obtained only at 700°C and $p/p^0 = 1$.

From the technological point of view, it is convenient to predict the appropriate initial gas phase composition giving rise to the required composition of solid nitride. Fig. 4 shows the input $x^0(\mathrm{TMA^{III}})$ inevitable for the composition $\mathrm{Ga}_y(\mathrm{Al}_{0.83}\mathrm{In}_{0.17})_{1-y}\mathrm{N}$, lattice matched to GaN at $t = 800°\mathrm{C}$, $p/p^0 = 1$ and V/III = 10000. The dependence of the initial gas phase ratio $x^0(\mathrm{TMAl})/x^0(\mathrm{TMIn})$ requisite for the solid nitride composition $x(\mathrm{AlN})/x(\mathrm{InN}) = 0.83/0.17$ is illustrated in Fig. 5. The sudden break on this curve corresponds to the composition $\mathrm{Ga}_{0.86}(\mathrm{Al}_{0.83}\mathrm{In}_{0.17})_{0.14}\mathrm{N}$. For values of $y < 0.86$, nitride is unstable and the phase separation occurs while homogeneous solid solution exists at $y > 0.86$. Another curve, calculated under the conditions when the solid nitride separation as well as the liquid phase formation are suppressed, is shown for comparison. The results demonstrate that increase of $x^0(\mathrm{TMGa})$ in the input gaseous phase leads to decrease of indium incorporation efficiency and lower values of $x^0(\mathrm{TMAl})/x^0(\mathrm{TMIn})$ are necessary to achieve the desired nitride composition.

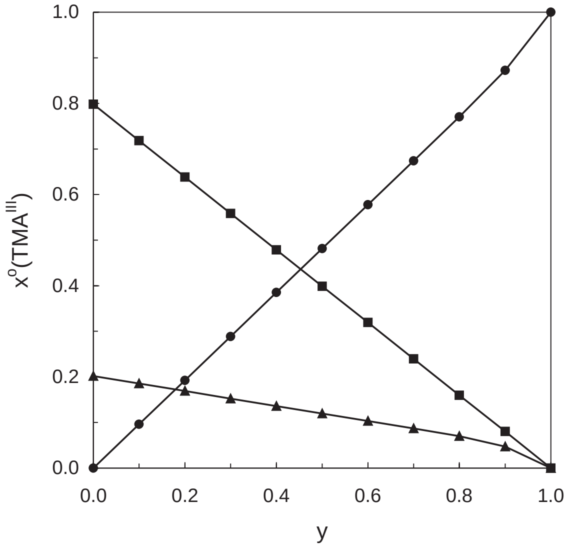

Fig. 4. Input molar fractions of $\mathrm{TMA^{III}}$ precursors, which give rise the composition $\mathrm{Ga}_y(\mathrm{Al}_{0.83}\mathrm{In}_{0.17})_{1-y}\mathrm{N}$, lattice matched to GaN at $t = 800°\mathrm{C}$, $p/p^0 = 1$, V/III = 10000, N_2 carrier gas, (■)—TMAl, (●)—TMGa, (▲)—TMIn.

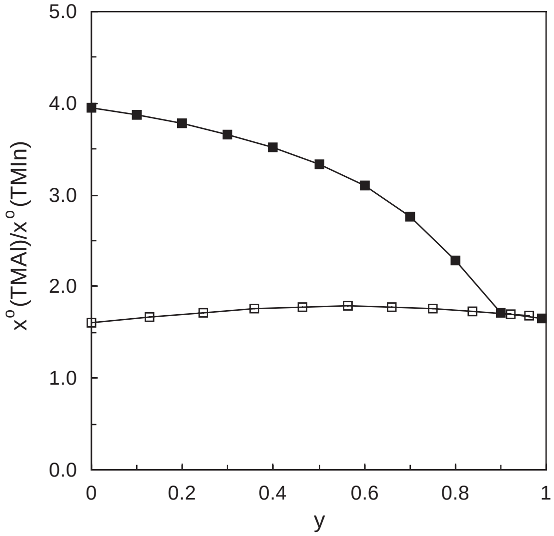

Fig. 5. Initial $x^0(\mathrm{TMAl})/x^0(\mathrm{TMIn})$ ratio requisite for the composition $\mathrm{Ga}_y(\mathrm{Al}_{0.83}\mathrm{In}_{0.17})_{1-y}\mathrm{N}$, lattice matched to GaN at $t = 800°\mathrm{C}$, $p/p^0 = 1$, V/III = 10000, N_2 carrier gas (full square—non-restricted equilibrium calculation, open square—solid nitride separation and liquid phase formation are suppressed).

Several studies dealing with the (Al,Ga,In)N epitaxial growth were published in literature [45–49]. The quality layers were prepared at temperatures 700–875°C under atmospheric or reduced pressure at V/III > 10^4 in nitrogen ambient using various A^{III} elements metalorganic precursors. The indium content ($x(\mathrm{InN})$) in the prepared layers was up to 0.38 at 700°C, up to 0.20 at 750–800°C and up to 0.10 at 875°C. These results generally correspond with our thermodynamic calculations.

Phase separation or composition fluctuations were observed in (Al,In)N [46,50], (Ga,In)N [51–53] and recently in (Al,Ga,In)N quaternary systems [54]. Limited miscibility of solid nitrides AlN, GaN and InN is also predicted by our thermodynamic calculations. This phenomenon is caused by the practically immiscible ternary system (Al,In)N.

As for the liquid phase formation, it was not reported for (Al,Ga,In)N growth till now. In case of (Ga,In)N, the In-rich metallic droplets were found on solid nitride surface at high input mole fraction of indium precursor and low values of V/III input ratio if the hydrogen was used as the carrier gas [55–57]. The In–N bond is relatively weak (in comparison with other A^{III} nitrides) which causes low stability of solid InN. As the vapor pressure of indium is very low at temperatures 750–850°C and no stable indium containing gaseous species exist in this system a liquid phase can be formed. The liquid phase formation is pronounced in the hydrogen atmosphere, presence of nitrogen suppresses the InN decomposition.

No systematic study on indium incorporation into solid (Al,Ga,In)N has been carried out yet and the indium content in the solid was fixed by the input mole fraction of indium precursor. On the other hand, this phenomenon has been studied in detail for the (Ga,In)N growth. In general, higher indium content in solid nitride can be achieved in nitrogen at lower temperatures (700°C). These experimental findings are also in qualitative agreement with our calculated results.

It is interesting to compare our results with those obtained by Koukitu at al. [24]. As there are large differences between our thermodynamic model and their quasi-thermodynamic treatment, the large disparity of the results exists, too. We believe that our approach is more reliable because it is possible to predict such phenomena as liquid droplets formation or composition fluctuations, which were observed experimentally during the epitaxial growth of indium containing A^{III} mixed nitrides. Moreover, the significant reduction of the number of gaseous phase components is baseless as a number of experimental as well as theoretical works exist, in which existence of various A^{III} gaseous substances was demonstrated. Some of the results of Koukitu et al. [24] are surprising and they should be discussed in more details. Unstability of aluminum-rich nitrides at higher temperatures and ambiguity of the solid nitride composition for the given input TMA^{III} mole fractions represent these cases in particular.

5. Conclusions

A detailed thermodynamic analysis was performed to predict suitable conditions for epitaxial growth of quaternary solid nitride (Al,Ga,In)N. As the quality of deposited layers is significantly influenced by liquid droplets formation, the operating temperature should be set at 700–850°C and nitrogen should be used as the carrier gas because no liquid phase is created under these conditions. There are large areas of coexistence of solid nitride and the liquid alloy in hydrogen ambient with the exception of the low temperature region (near 700°C). Indium incorporation is affected by the nature of the carrier gas, too. Sufficiently high content of indium in solid nitride can be achieved only in nitrogen at temperatures 700–800°C under atmospheric or slightly reduced pressures ($p/p^0 = 0.1$). Indium incorporation efficiency decreases with increasing temperature and decreasing pressure. As it was already mentioned our thermodynamic calculations are in qualitative agreement with majority of the experimental findings on (Al,Ga,In)N, (Al,In)N and (Ga,In)N epitaxial growth. On the other hand, there are significant differences between the presented results and results from quasi-equilibrium calculations by Koukitu et al. [24].

Acknowledgements

This work was supported by the Grant Agency of the Czech Republic (grant No. 104/03/0387) and the Ministry of Education of the Czech Republic research project No. 223400008).

References

[1] B. Monemar, J. Mater. Sci. Mater. Electron. 10 (1999) 227.
[2] P. Kung, M. Razeghi, Opto-Electron. Rev. 8 (2000) 201.
[3] B. Monemar, G. Pozina, Prog. Quantum Electron. 24 (2000) 239.

[4] A.G. Thompson, Mater. Lett. 30 (1997) 255.

[5] W.G. Breiland, M.E. Coltrin, J.R. Creighton, H.Q. Hou, H.K. Moffat, J.Y. Tsao, Mater. Sci. Eng. R 24 (1999) 241.

[6] S. Pellegrino, L. Tarricone, Mater. Chem. Phys. 66 (2000) 189.

[7] G.B. Stringfellow, J. Crystal Growth 62 (1983) 225.

[8] G.B. Stringfellow, J. Crystal Growth 70 (1984) 133.

[9] A. Koukitu, N. Takahashi, H. Seki, Jpn. J. Appl. Phys. 36 (Part 2) (1997) L1136.

[10] J. Leitner, J. Stejskal, P. Voňka, Mater. Lett. 28 (1996) 197.

[11] C. Li, Z. Du, W. Zhang, CALPHAD 24 (2000) 169.

[12] A. Koukitu, H. Seki, Jpn. J. Appl. Phys. 35 (Part 2) (1996) L1638.

[13] D. Lu, S. Duan, Chin. J. Semicond. 20 (1999) 1026.

[14] J. Leitner, J. Stejskal, P. Voňka, Chem. Listy 94 (2000) 947.

[15] D. Lu, S. Duan, J. Crystal Growth 208 (2000) 73.

[16] A. Koukitu, Y. Kumagai, H. Seki, Phys. Stat. Sol. (a) 180 (2000) 115.

[17] D. Lu, S. Duan, Chin. J. Semicond. 21 (2000) 729.

[18] A. Koukitu, N. Takahashi, T. Taki, H. Seki, Jpn. J. Appl. Phys. 35 (Part 2) (1996) L673.

[19] A. Koukitu, N. Takahashi, T. Taki, H. Seki, J. Crystal Growth 170 (1997) 306.

[20] A. Koukitu, H. Seki, J. Crystal Growth 189/190 (1998) 13.

[21] J. Leitner, J. Stejskal, Mater. Lett. 35 (1998) 85.

[22] T. Asai, D.S. Dandy, J. Appl. Phys. 88 (2000) 4407.

[23] D. Lu, S. Duan, Chin. J. Semicond. 21 (2000) 105.

[24] A. Koukitu, Y. Kumagai, H. Seki, J. Crystal Growth 221 (2000) 743.

[25] P. Voňka, J. Leitner, CALPHAD 19 (1995) 25.

[26] M. Tirtowidjojo, R. Pollard, J. Crystal Growth 77 (1986) 200.

[27] O. Knacke, O. Kubaschewski, K. Hesselmann, Thermochemical Properties of Inorganic Substances, 2nd Edition, Springer, Berlin, 1991.

[28] E.J. Abril, A. Alonso, M. Lopez, M. Aguilar, Inst. Phys. Conf. Ser. 129 (Gallium Arsenide and Related Compounds, 1992), Inst. Phys., 1993, p. 121.

[29] I. Ansara, C. Chatillon, H.L. Lukas, T. Nischizawa, H. Ohtani, K. Ishida, M. Hillert, B. Sundman, B.B. Argent, A. Watson, T.G. Chart, T. Anderson, CALPHAD 18 (1994) 177.

[30] I.N. Przhevalskii, S.Yu. Karpov, Yu.N. Makarov, MRS Internet J. Nitride Semicond. Res. 3 (1998) 30.

[31] A.T. Dinsdale, CALPHAD 15 (1991) 317.

[32] A.V. Davydov, T.J. Anderson, Proc. Electrochem. Soc., 98-18 (III–V Nitride Materials and Processing), Electrochem. Soc., 1999, p. 38.

[33] I. Barin, Thermochemical Data of Pure Substances, 2nd Edition, VCH, Weinheim, 1993.

[34] M.R. Ranade, F. Tessier, A. Navrotsky, V.J. Lepper, S.H. Risbud, F.J. DiSalvo, C.M. Balkas, J. Phys. Chem. B 104 (2000) 4060.

[35] T. Matsuoka, Appl. Phys. Lett. 71 (1997) 105.

[36] T. Matsuoka, J. Crystal Growth 189/190 (1998) 19.

[37] T. Matsuoka, MRS Internet J. Nitride Semicond. Res. 3 (1998) 54.

[38] E.N. Vigdorovich, Yu.N. Sveshnikov, Inorg. Mater 36 (2000) 465.

[39] T. Takayama, M. Yuri, K. Itoh, T. Baba, J.S. Harris Jr., J. Crystal Growth 222 (2001) 29.

[40] J. Leitner, J. Phys. Chem. Solids 58 (1997) 1329.

[41] M. van Schilfgaarde, A. Sher, A.B. Chen, J. Crystal Growth 178 (1997) 8.

[42] T. Saito, Y. Arakawa, Phys. Rev. B 60 (1999) 1701.

[43] T. Ito, Phys. Stat. Sol. (b) 217 (2000) R7.

[44] L.K. Teles, J. Furthmüller, L.M.R. Scolfaro, J.R. Leite, F. Bechstedt, Phys. Rev. B 62 (2000) 2475.

[45] F.G. McIntosh, K.S. Boutros, J.C. Roberts, S.M. Bedair, E.L. Piner, N.A. El-Masry, Appl. Phys. Lett. 68 (1996) 40.

[46] S. Yamaguchi, M. Kariya, S. Nitta, H. Kato, T. Takeuchi, C. Wetzel, H. Amano, I. Akasaki, J. Crystal Growth 195 (1998) 309.

[47] M.E. Aumer, S.F. LeBoeuf, F.G. McIntosh, S.M. Bedair, Appl. Phys. Lett. 75 (1999) 3315.

[48] J. Han, J.J. Figiel, G.A. Petersen, S.M. Myers, M.H. Crawford, M.A. Banas, Jpn. J. Appl. Phys. 39 (Part 1) (2000) 2372.

[49] J. Li, K.B. Nam, K.H. Kim, J.Y. Lin, H.X. Jiang, Appl. Phys. Lett. 78 (2001) 61.

[50] S. Yamaguchi, M. Kariya, S. Nitta, T. Takeuchi, C. Wetzel, H. Amano, I. Akasaki, Appl. Phys. Lett. 76 (2000) 876.

[51] H.K. Cho, J.Y. Lee, K.S. Kim, G.M. Yang, J. Crystal Growth 220 (2000) 197.

[52] D. Gerthsen, E. Hahn, B. Neubauer, A. Rosenauer, O. Schön, M. Heuken, A. Rizzi, Phys. Stat. Sol. (a) 177 (2000) 145.

[53] A. Kaschner, A. Hoffmann, C. Thomsen, T. Böttcher, S. Einfeldt, D. Hommel, Phys. Stat. Sol. (a) 179 (2000) R4.

[54] Y. Kobayashi, Y. Yamauchi, N. Kobayashi, Jpn. J. Appl. Phys. 42 (2003) 2300.

[55] M. Shimizu, K. Hiramatsu, N. Sawaki, J. Crystal Growth 145 (1994) 209.

[56] H. Lu, M. Thothathiri, Z. Wu, I. Bhat, J. Electron. Mater. 26 (1997) 281.

[57] S. Keller, B.P. Keller, D. Kapolnek, U.K. Mishra, S.P. DenBaars, I.K. Shmagin, R.M. Kolbas, S. Krishnankutty, J. Crystal Growth 170 (1997) 349.